

# Positions of cut lines of the superlogarithm

Dmitrii Kouznetsov

(Inst.for Laser Science, Univ.of Electro Communications, 182-8585, Japan)

Henryk Trappmann

March 28, 2009

## Abstract

The superexponential and the modified superlogarithm of a complex argument show quasiperiodic self-similar structures.

Keywords: tetration, superexponential, superlogarithm, branch points, cut lines, self-similarity

## 1 Introduction

The super-exponential  $\text{sexp}$  can be defined as the holomorphic extension of a function of the integer argument, that produces the sequence

$$0, 1, e, \exp(e), \exp(\exp(e)), \dots, \exp^N(0) = \text{sexp}(N), \dots \quad (1)$$

From the integer number  $N$  of iteration of the exponential, it is extended to real and complex values [1, 2, 3]. This extension is similar to the holomorphic extension of the sequence of sums of the arithmetic progression

$$0, 1, 1+2, 1+2+3, \dots, f(N) = N(N+1)/2, \dots \quad (2)$$

or the sequence of partial sums of the geometric progression

$$1, 1+r, 1+r+r^2, \dots, f(N) = (r^{N+1}-1)/(r-1), \dots \quad (3)$$

or the products of natural numbers

$$1, 1 \times 2, 1 \times 2 \times 3, \dots, f(N) = N!, \dots \quad (4)$$

initially defined for a positive integer  $N$ . Some textbooks [4] assume, that factorial is defined only for integer values of the argument; notation  $\Gamma(N+1)$  is used instead of  $N!$  for the cases of a non-integer  $N$ . On the other hand, various competing mathematical software (Mathematica, Maple) recognize  $N!$  as holomorphic function, allowing the integration, differentiation, asymptotical expansion, expression through other functions and plotting in the complex plane; there is no need to make any difference between  $N!$  and  $\Gamma(N+1)$  for complex  $N$ .

The uniqueness of the extension of a function of integer variable could be provided by the requirements about the behavior of this function in the complex plane. For example, in the case of the arithmetic progression, the modification  $f(z) \rightarrow f(z + \alpha \cdot \sin(2\pi z))$  leads to a function with an exponential growth in the direction of the imaginary axis; there is only one extension with slower than exponential growth; similarly, one could consider  $f(z) + \alpha \cdot \sin(2\pi k z)$  for integer  $k$  and some  $\alpha$ .

The analytic properties of holomorphic extensions of tetration were analyzed since the past century. The existence of a holomorphic superexponential was analyzed in [5]. The uniqueness of the biholomorphic pair (sexp,slog) is demonstrated in [6]. The algorithm for the precise evaluation of the superexponential (holomorphic tetration) through the Cauchi contour integral is suggested in [7]; and it is declared (without proof), that the superexponential  $f = \text{sexp}$  is unique holomorphic solution of the eqs.

$$\exp(f(z)) = f(z+1) \quad \forall z \in C = \mathbb{C} \setminus \{x \in \mathbb{R} : x \leq -2\}, \quad f(0) = 1, \quad (5)$$

that approaches its limiting values  $L, L^*$  at  $z = x \pm i\infty$  for all real  $x$ .

Function  $f = \text{sexp}(z)$  in the complex  $z$ -plane is plotted in the left hand side picture of the figure 1. Levels of constant  $u = \Re(f)$  and levels of constant  $v = \Im(f)$  are drawn. The right hand side picture shows the inverse function  $f = \text{slog}(z)$  in the same notations;

$$\text{sexp}(\text{slog}(z)) = z; \quad (6)$$

The levels of integer values of  $u$  and  $v$  are shown with thick solid lines. The intermediate levels are shown with thin lines. In the case of sexp, the light thick dashed lines show the additional levels  $u = \Re(L)$  and  $v = \pm \Im(L)$ , where  $L \approx 0.3 + 1.3i$  is fixed point of logarithm;  $L = \log(L)$ . The black dashed lines show the cuts of the range of holomorphism.

The plot of sexp reveals the quasiperiodicity;

$$f(z) \approx f(z+T) \quad \text{at} \quad \Im(z) > 1, \quad (7)$$

$$f(z) \approx f(z+T^*) \quad \text{at} \quad \Im(z) < 1. \quad (8)$$

where  $T = 2\pi i / L \approx 4.447 + 1.058i$ . This quasiperiodicity allows the fast and precise evaluation of sexp at large values of the imaginary part of the argument.

In addition to the quasiperiodicity (7), the function sexp shows also another kind of symmetry. The levels  $\Im(\text{sexp}(z))$  are reproduced at the translations  $z \rightarrow z+1$ . In this paper, we analyze this property and show that it is related to the fractal character of zeros of the imaginary part of the superexponential.

## 2 Approximation

For creation of the detailed plots of the sexp, the superexponential [7] was evaluated through the solution  $f$  of the integral eq.

$$f(z) = \frac{1}{2\pi} \int_{-A}^A \frac{\exp(f(ip)) dp}{1 + ip - z} - \frac{1}{2\pi} \int_{-A}^A \frac{\ln(f(ip)) dp}{-1 + ip - z} + \mathcal{K}(z), \quad (9)$$

$$\mathcal{K}(z) = L \left( \frac{1}{2} - \frac{1}{2\pi i} \ln \frac{1 - iA + z}{1 + iA - z} \right) + L^* \left( \frac{1}{2} - \frac{1}{2\pi i} \ln \frac{1 - iA - z}{1 + iA + z} \right) \quad (10)$$

at  $A \gg 1$ . Through this solution, the Taylor expansions [8, 9] were calculated. Similar approximation can be used for slog. These approximations have the same precision, as the evaluation through the contour integral, but the expansions run significantly faster, than the integrals.

### 3 Self-similar behavior of superexponential

In addition to the quasi-periodicity (7), some self-similarity at the unity translations is seen in the plot of  $\text{sexp}$  in Figure 1: the line  $\Im(\text{sexp}(z)) = 0$  reproduces again and again at the translations  $z \rightarrow z + 1$ . Also, the superexponential shows complicated behavior and looks chaotic in the range  $\Re(Lz) > 0, \Re(L^*z) > 0$  of the complex  $z$  plane, and, in particular, in vicinity of the positive part of the real axis. This function makes the impression of a fractal object. On the other hand, the superexponential is holomorphic at  $\Re(z) > 0$ ; so, it is completely regular there. In order to resolve this paradox, consider the set

$$F = \{ z \in \mathbb{C} : \exists n \in \mathbb{N} : \Im(\text{sexp}(z+n)) = 0 \} \quad (11)$$

The fig. 2 somehow illustrates this set.

The plotting of a fractal object is always a compromise, while the set has measure zero, but is dense everywhere in the complex plane. If we put a pixel in vicinity of each point that belongs to the set  $F$ , then the image looks like a “Black Square” by Kazimir Malevich. One could choose some set of points (for example, the rectangular mesh), and mark with black pixel all points, that belong to  $F$ . In this case, the most of the picture remains white. In any of these extreme cases, the plot brings no information about structure of the fractal object. As a compromise, the fig. 2 shows the zoom from fig. 1, with extended lines of level  $\Im(\text{sexp}(z)) = 0$ . In addition, in fig. 2, the regions  $|\Im(\text{sexp}(z))| < 10^{-12}$  are shaded. This plot can be considered as an “approximation” of the fractal  $F$ ;

$$F_n = \{ z \in \mathbb{C} : \Im(\text{sexp}(z+n)) = 0 \} \quad \forall n \in \mathbb{N} . \quad (12)$$

Due to relation  $\text{sexp}(z+1) = \exp(\text{sexp}(z))$ , the increase of  $n$  only add new elements to the set; each next elements of the sequence of these approximations includes the previous one:  $F_n \subset F_{n+1}$ . At the bottom of the fig., many pixels are plotted, and the pattern looks quasi-periodic with period unity. This explains the quasi-periodic behavior of the superexponential in vicinity of the real axis; only the imaginary part of the function shows this quasi-periodicity.

At relatively moderate values  $\Re(z) \approx 8$ , it is already impossible to draw all the lines  $\Im(\text{sexp}(z)) = 0$  in the graphic. Even worse; in the field of fig. 2, in some regions, at the complex (double) precision, it is not possible to distinguish values of the superexponential from infinity. These regions are left blank. Together with the regions, where the imaginary part is not distinguishable from zero (marked with black), these white regions form the zebra-like structure of self-similar black and white strips. In this sense, the “approximation”  $F_n$  by (12) already looks as a fractal object at  $n = 8$ . The precision of evaluation of the superexponential allows to trace these fringes until the appearance of the Moire fringes at the overlapping of the quasi-periodic structure with the discrete sampling at the plot of the figure; in particular, the

2000x2000 array is used to sample the function in order to plot the Figure 2, and the star-like Moire structures become seen at the zooming-in.

In the limit  $n \rightarrow \infty$ , the set  $F_n$  becomes periodic; however, a perfect drawing becomes impossible because in vicinity of each point  $z$ , there exist points that belong to  $F$  and there exist points that do not. Such a fractal behavior is typical for reiterations of holomorphic functions. In this sense, the set of zeros of the imaginary part of the superexponential can be considered as a fractal object.

## 4 Modified superexponential

Various other fractal objects can be constructed on the base of the superexponential. In particular, the singularities of the superexponential with the modified argument

$$f(z) = \text{sexp} \left( z + \sum_n \alpha_n \sin(2\pi n z) + \sum_n \beta_n (1 - \cos(2\pi n z)) \right). \quad (13)$$

also form self-similar quasiperiodic structures, while any of  $\alpha$  or  $\beta$  is different from zero; although these singularities may be not dense, as the set  $F$  by (11) is. For small values of  $\alpha$  and  $\beta$ , the modified superexponential (13) satisfies the same eqs. as the superexponential,  $f(z+1) = \exp(f(z))$ ,  $f(0) = 1$ ; at least in some vicinity of the real axis. As an example of such functions, in fig. 3, the function  $f$  is plotted at  $\alpha_1 = 10^{-4}$ ,  $\alpha_n = 0$  at  $n > 1$  and  $\beta_n = 0$  for all  $n$ . The left hand side picture, the scale is the same, as in fig. 1; the right hand side represents the 5x zoom of the region with left bottom corner at  $z = i$ . In vicinity of the real axis, the deviation from the left hand side picture in fig. 1 is not visible. At  $\Im(z) > 2$ , the density of levels becomes high and the plotter cannot plot them. In vicinity of the lines  $\Im(z + 0.0001 \sin(2\pi z)) = 0$ , the modified tetration shows the additional cuts and rapid growth, dependent on the values of  $\Re(z + 0.0001 \sin(2\pi z))$ , producing the self-similar structures. The zoom-in of such structures is seen at the zooming-in in the right hand side of the picture. Similar pictures can be plotted for other values of  $\alpha$  and  $\beta$ .

The absence of the singularities (except at integer values  $n < -1$ ) could be considered as a criterion of the uniqueness of the holomorphic superexponential. In such a way, the holomorphic superexponential produces the simplest fractal among various solutions of the eq. of tetration with reduced range of holomorphy.

## 5 Cutlines of slog

The self-similar structures can be made also from the function slog. There is some freedom to choose the cut lines of the slog function. In fig. 1, the cuts are placed along the lines  $\Re(z) < \Re(L)$ ,  $\Im(z) = \pm \Im(L)$ . An alternative of the slog is plotted in the left hand side picture in fig. 4, with cuts are placed along the lines  $\Re(z) > \Re(L)$ ,  $\Im(z) = \pm \Im(L)$ . In the central part,  $|\Im(z)| < \Im(L)$ , this picture coincide with plot of slog in the fig. 1.

The “alternative” slog function, shown in fig. 4, is evaluated using the same approximation in the basic region

$$G = \{ z \in \mathbb{C} : \Re(z) > \Re(L), |z| < |L| \} \quad (14)$$

The region  $G$  and its image  $\text{slog}(G)$  are shaded in figs. 1 and 4. Then, the approximation can be extended to the whole complex plane, using relations

$$\text{slog}(z) = \text{slog}(\exp(z)) - 1 \quad \text{or} \quad (15)$$

$$\text{slog}(z) = \text{slog}(\log(z)) + 1 \quad (16)$$

There is an important question, which of these two formulas should be applied for the evaluation of  $\text{slog}(z)$  at  $|\Im(z)| > \Im(L)$ . For the  $\text{slog}$ , shown in fig. 1, formula (16) is used; in this case, the cut lines are just cut lines of the logarithmic function, shifted to the fixed points  $L$  and  $L^*$ .

The picture in the upper left corner of the fig. 4 represents the modified  $\text{slog}$  function. For this modified function, the relation (15) is used, if  $|\Im(z)| > \Im(L)$ . In this case, the basic cut lines from the branch points are directed to the right. As the first operation is the exponentiation, the periodicity takes place; the modified  $\text{slog}$ , evaluated at  $z + 2\pi i$ , is the same, as the modified  $\text{slog}$ , evaluated at  $z$ . In this case, the additional branch points appear; they form complicated self-similar fractal structure. Two sequential zooms of the modified  $\text{slog}$  function are shown in the bottom and the upper-right pictures of the fig. 4. The set  $S$  of the branchpoints can be successively constructed as follows:

$$S \subset \{ L_n, L_n^*; n \in \mathbb{N} : n \geq 0 \} \quad (17)$$

$$S = S \cup \{ \log(z) + 2\pi im; z \in S, m \in \mathbb{N} : |\Im(\log(z)) + 2\pi m| > \Im(L_0) \} , \quad (18)$$

where  $L_m$  is fixed point of the exponential,

$$L_m = \log(L_m) + 2\pi im ; \quad (19)$$

and  $\Im(L_0) > 0$ . Equation (18) determines the straightforward iterational procedure to calculate the branchpoints of the modified  $\text{slog}$ ; the set  $S$  is countable and is not dense at any region of the complex plane. In particular, the first row of the branchpoints in the fig. 4 begins with

$$\begin{aligned} s_{0,0} &= L_0 = L \approx 0.3181315052047641353 + 1.3372357014306894089 i , \\ s_{0,1} &= \log(L^* + 2\pi i) \approx 1.6006333482537577368 + 1.5065631897208156242 i \\ s_{0,2} &= \log(L + 2\pi i) \approx 2.0317022759689103667 + 1.5290733194545589200 i \quad (20) \\ s_{0,3} &= \log(L^* + 4\pi i) \approx 2.4189128911991812305 + 1.5424730023695385445 i \\ s_{0,4} &= \log(L + 4\pi i) \approx 2.6324099603270543794 + 1.5479190965188477614 i \end{aligned}$$

The appearance of the additional branch points makes the modified  $\text{slog}$  function more complicated, than just  $\text{slog}$ . This is serious reason in favor of just  $\text{slog}$  (and not modified  $\text{slog}$ ) function in the definition (and evaluation) of the generalized exponential

$$\exp^c(z) = \text{sexp}(c + \text{slog}(z)) . \quad (21)$$

This function is plotted in the left hand side picture of fig. 5 for  $c = 1/2$ , in the same notations, as in fig. 1. The existence of holomorphic  $\sqrt{\exp}$  was shown in the past century [5], but not so many plots of this function are available in the publications, if at al. The generalized exponential can be evaluated by (21) for various values  $c$ . The right hand side of fig. 5 represents the similar plot for the generalized exponential with  $\text{slog}$  replaced to modified  $\text{slog}$ ; in this case,

the additional cut lines divide the range of holomorphism to the separated strips. The plots are symmetric, so, the only upper part of the complex plane is shown. In vicinity of the real axis, in the strip  $|\Im(z)| < \Im(L)$ , the  $\text{slog}(z)$  and its modification are the same; therefore, the bottom part of the plots of generalized exponential and its modification is the same; the fractal behavior appears only at  $|\Im(z)| > \Im(L)$ .

For the simplest functions, the  $\text{slog}(z)$  should have cuts along the lines  $\Re(z) < \Re(L)$ ,  $\Im(z) = \pm\Im(L)$ , as it is shown in the right hand side of the fig.1. In such a way, the analysis of the fractal structure of the inverse function of the superexponential gives the criterion in the choice of the cuts of the range of the holomorphism.

## 6 Conclusions

The superexponential has two kinds of quasi-periodicity. The first corresponds to the translations with quasi-period  $T = 2\pi i/L$  in the upper half-plane and  $T^*$  in the lower half-plane; both real and imaginary parts of the function are asymptotically reproduced at these translations. The second kind of quasi-periodicity corresponds only to the imaginary part of the function; at the unity translations along the real axis, the elements of the fractal  $F$  by (11) remains at their places.

The superlogarithm is a regular and smooth function, but at the rotation of the cut lines for an angle  $\pi$  clock-vice in the upper half-plane and counter-clock vice in the lower half-plane, the self-similar structures of the cut lines appear; these structures also look like a fractal. Such a fractal behavior of superlogarithm with alternative position of cut lines should be considered as an argument in favor of the left-going cut lines, as they are shown in the right hand side of the fig. 1. This reason should be taken into account for the implementation of the superlogarithm in mathematical software.

The fractal structure of the modified superlogarithm (Figure 3) allows the variety of another fractal functions; in particular, the modifications of the generalised exponentiation (21). The fractal behavior is not specific for the  $\text{sexp}$  at the base  $e$ ; it takes place also for the holomorphic tetration of other bases and, in particular, the holomorphic extension of the Ackermann functions [10, 11, 12], which corresponds to base 2.

## References

- [1] N.Bromer. Superexponentiation. *Mathematics Magazine*, **60** No. 3 (1987), 169-174.
- [2] A.Knoebel. Exponentials Reiterated. *Amer. Math. Monthly* **88** (1981), 235-252.
- [3] P.Walker. Infinitely differentiable generalized logarithmic and exponential functions. *Mathematics of computation*, **196** (1991), 723-733.
- [4] M.Abramowitz, I.Stegun. Handbook on mathematical functions. NY, 1967
- [5] H.Kneser. Reelle analytische Lösungen der Gleichung  $\varphi(\varphi(x)) = e^x$  und verwandter Funktionalgleichungen. *Journal für die reine und angewandte Mathematik*, **187** (1950), 56-67.

- [6] H.Trappmann, D.Kouznetsov. Uniqueness of Holomorphic superlogarithms, *Functional analysis and its applications*, under consideration.
- [7] D.Kouznetsov. Solutions of  $F(z+1)=\exp(F(z))$  in complex  $z$ -plane. *Mathematics of computation*, (2009) in press  
<http://www.ams.org/mcom/0000-000-00/S0025-5718-09-02188-7/home.html>
- [8] D.Kouznetsov. Examples of the complex implementation of the superexponential <http://en.citizendium.org/wiki/TetrationDerivativesReal.jpg/code> and the superlogarithm <http://en.citizendium.org/wiki/SLOGappro50.jpg/code> through the Taylor expansions.
- [9] D.Kouznetsov. Superexponential as special function. preprint ILS, 2009, in preparation.
- [10] W.Ackermann. Zum Hilbertschen Aufbau der reellen Zahlen. *Mathematische Annalen* **99**(1928), 118-133.
- [11] D.Kouznetsov. Portrait of the analytic extension of the 4th Ackermann function in the complex plane. <http://en.citizendium.org/wiki/Image:Analytic4thAckermannFunction00.jpg>
- [12] <http://en.citizendium.org/wiki/Tetration>

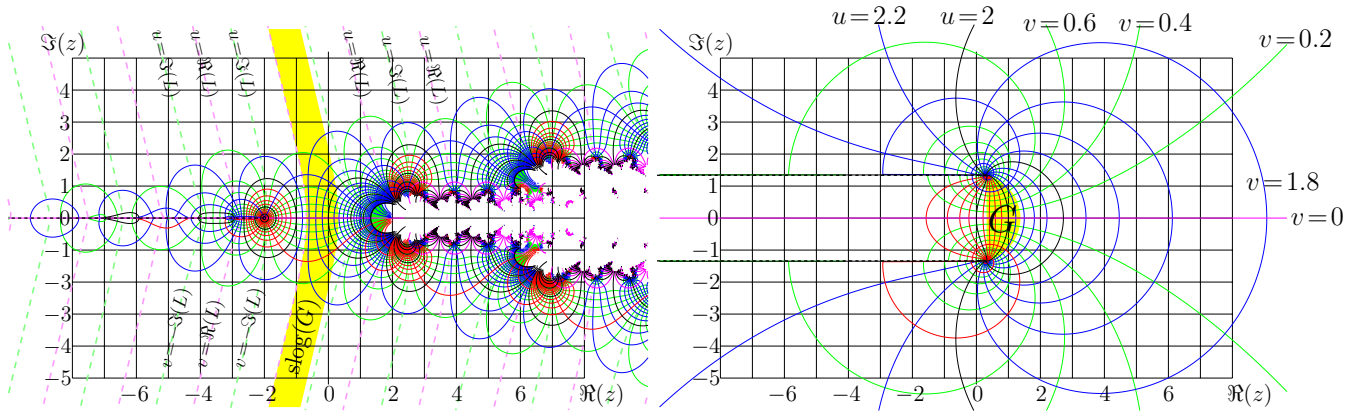


Figure 1: functions  $f = \text{sexp}(z)$ , left, and  $f = \text{slog}(z)$ , right, in the complex  $z$ -plane.

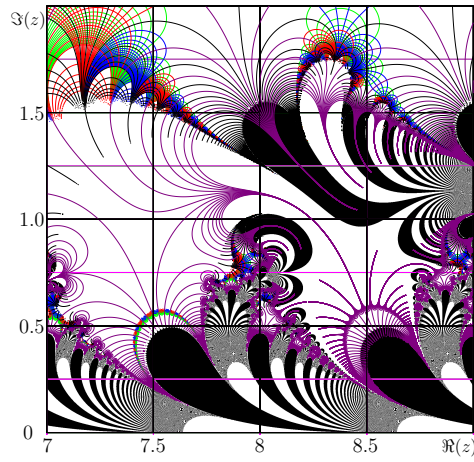


Figure 2: Zoom-in from figure 1, with shaded regions  $|\Im(\text{sexp}(z))| < 10^{-12}$ .

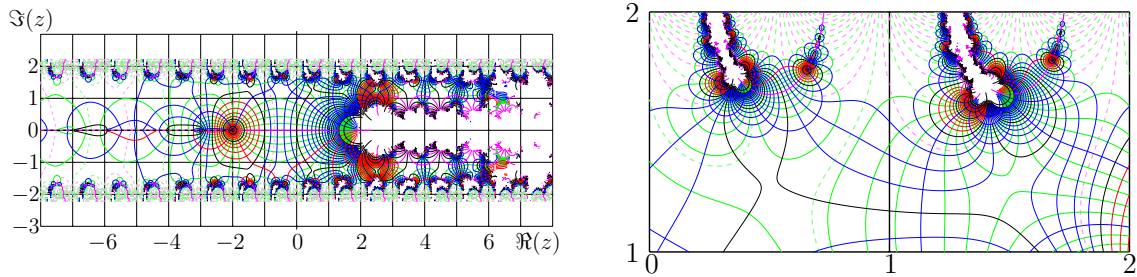


Figure 3: Example of the modified superexponentiation by (13) in the complex plane.

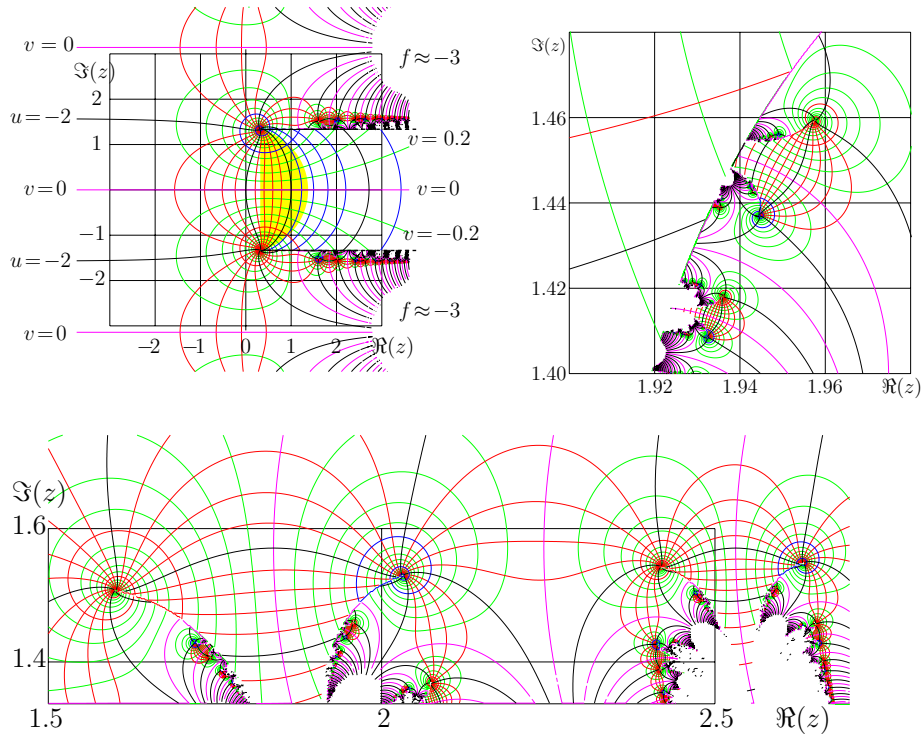


Figure 4: Alternative of function slog (see fig.1) with opposite direction of the cut lines, upper left picture. The zoom-in of the region just above the upper straight cut line, bottom. The zoom-in of the region in vicinity of the additional cut line, upper right corner.

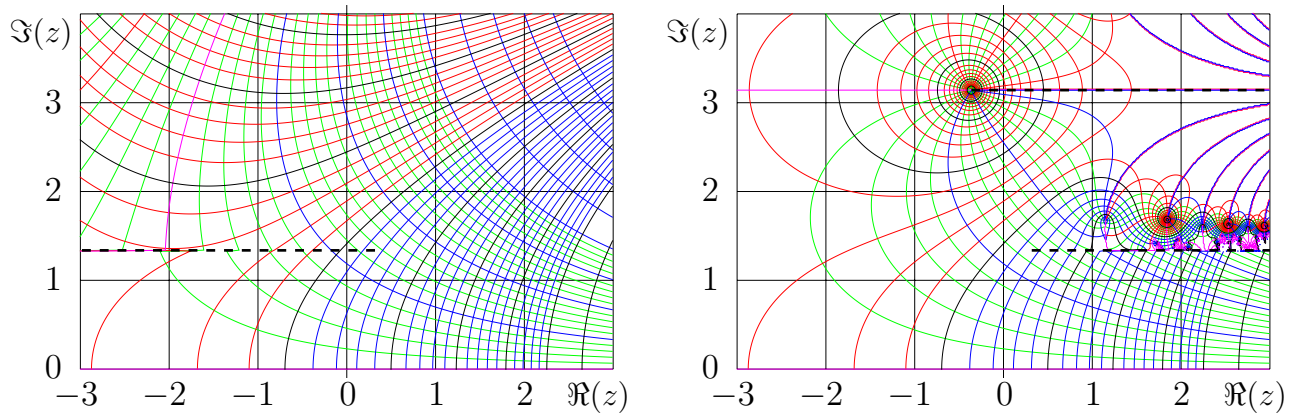


Figure 5:  $\sqrt{\exp}(z)$  by (21) in the complex  $z$  halfplane (left) and its modification (right).